NASA Technical Paper 3635

1996

Photovoltaic Plasma Interaction Test II

Bradford A. Kaufman and Daniel Chrulski
Lewis Research Center
Cleveland, Ohio

Roger M. Myers
NYMA, Inc.
Brook Park, Ohio

National Aeronautics and
Space Administration
Office of Management
Scientific and Technical
Information Program

Photovoltaic Plasma Interaction Test II

Bradford A. Kaufman and Daniel Chrulski
National Aeronautics and Space Administration
Lewis Research Center
Cleveland, Ohio 44135

and

Roger M. Myers
NYMA, Inc.
Brook Park, Ohio 44142

Summary

The International Space Station (ISS) program is developing a plasma contactor to mitigate the harmful effects of charge collection on the station's large photovoltaic arrays.

The purpose of the present test was to examine the effects of charge collection on the solar array electrical circuit and to verify the effectiveness of the plasma contactor. The results showed that the plasma contactor was able to eliminate structure arcing for any array output voltage. However, the current requirements of the plasma contactor were higher than those measured during prior testing and predicted by analysis. Three possible causes for this excess current demand are discussed. The most likely appeared to be a high local pressure on or very near the surface of the array as a result of vacuum tank conditions. Therefore, in actual space conditions, the plasma contactor should work as predicted.

Introduction

The International Space Station (ISS), similar to the Space Station Freedom (SSF) that it replaced, will operate in low-Earth orbit (LEO) at an altitude of 330 to 460 km. The space environment at this altitude is primarily neutral monatomic oxygen, created by photodissociation of residual oxygen molecules from the Earth's atmosphere, positively charged oxygen ions, and negatively charged electrons. This "cloud" of electrons, ions, and atoms is called plasma. With the inclusion of the Russian Space Agency in the ISS program, the ISS's orbital inclination was changed from 28.5° to 51.6°, which slightly decreased electron density in the sunlit portion of the orbit and slightly increased it in the eclipse portion. Calculations show that the maximum electron density of 3.3×10^6 electrons/cm^3 occurs during a winter solar maximum whereas the maximum electron temperature of 0.27 eV occurs during a summer solar maximum (Private communication with David B. Snyder, NASA Lewis Research Center, Cleveland, Ohio, Sept. 8, 1994.). While on-orbit, the ISS's movement through the space plasma generates electrical potentials, which result from the difference in charge between the station and the charged particles of the plasma. The station's charge is generated by the photovoltaic arrays (which operate nominally at 160 V) and the negative grounding scheme that "floats" the station's structure to a potential of approximately –140 V relative to the plasma. This floating potential causes the collection of electrons by the uninsulated cell edges of the photovoltaic arrays and ions by the station's structure. When the collected charges are sufficient, the established localized potential causes the station's surfaces to undergo dielectric breakdown (i.e., arcing), resulting in material damage and electromagnetic interference. A device called the plasma contactor will be used to reduce the harmful effects caused by the floating potential. The plasma contactor provides a low-impedance current path to the plasma, thus draining off station charge and elevating the floating potential towards 0 V.

The purposes of this test were to investigate the effects of a plasma environment on an ISS solar array circuit and to confirm the results of a prior photovoltaic plasma interaction test (PVPIT I) (ref. 1). PVPIT I was conducted with development panels and used the SSF 28.5° orbit inclination and plasma conditions. Another purpose of the present test was to evaluate the effectiveness of the plasma contactor in neutralizing the collected charges. The solar array in this test had two flight-quality panels connected by a flat collector circuit (FCC). Each panel was composed of two hundred 8×8 photovoltaic cells with bypass diodes connected across every eight cells. To enhance the systems aspects of the test, a circuit with frequency and filter characteristics similar to those of the sequential shunt unit (SSU) was used for switching (i.e., shorting) the array. In addition, a breadboard plasma contactor and the three-bay FASTMast (folding articulated square truss mast) were included in the solar array circuit during testing. This test also used a flight-quality temperature sensor (the type scheduled to be flown on Mir) to obtain high-fidelity temperature data, which will be used to compare the flight temperature sensors to standard thermocouples and to verify math models that are used to predict solar array on-orbit performance.

The objectives of the PVPIT II were to

1. Confirm the floating potential and current collected by a single solar array circuit of flight-qualification fidelity at expected operating parameters in a simulated space plasma environment.
2. Confirm the dynamic behavior of the same circuit operating during switching.
3. Confirm the operating margin with respect to current collection and arcing.
4. Confirm the floating potential shift and operating parameters of a plasma contactor electrically connected to the photovoltaic (PV) array circuit.
5. Observe the floating behavior of a FASTMast section electrically connected to the PV panel.
6. Obtain high-fidelity temperature data of the solar array.

The appendix lists the acronyms used in this report.

Test Equipment and Environment

Environmental Systems

Vacuum facility.—The PVPIT II was conducted in the NASA Lewis Research Center Electric Propulsion Laboratory's tank 5 vacuum facility, which is 15 ft (4.6 m) in diameter and 60 ft (18.3 m) in length. Approximately half the tank was occupied by the test cage assembly. The vacuum pumping system consisted of mechanical roughing pumps, a Roots-type blower, and 20 oil diffusion pumps. In addition, a liquid helium cryopanel was used to increase the pumping speed when the plasma sources were used. This cryopanel was located inside the tank and occupied the other half. Vacuum levels achieved were on the order of 10^{-6} N/m^2 prior to testing and 10^{-5} N/m^2 during testing.

Test cage assembly (TCA).—The test cage assembly, an octagonal aluminum structure 14 ft (4.3 m) high, 12 ft (3.7 m) wide, and 17 ft (5.2 m) long, supported the hanging solar array, a solar simulator (the lamp bank), a cooling source (the cold wall), the plasma sources, and the plasma diagnostic probes (fig. 1).

Lamp bank: The lamp bank, or solar simulator, provided an average intensity of 0.38 suns at the surface of the solar array (66 in. or 167.6 cm from array to lamp bank). The simulator consisted of 252 ANSI-type "DED" multimirror General Electric 85-W quartz lamps that were arranged in 7 horizontal rows spanning 184 in. (467.4 cm) and 72 vertical rows spanning 30 in. (76.2 cm). The spacing between the lamps was 5.25 in. (13.3 cm) in the horizontal direction and a nominal 5 in. (12.7 cm) in the vertical direction.

The lamps were wired in nine series, parallel groups to achieve uniform intensity. Each group was independently controlled by a constant voltage dc power supply. This configuration made it possible to apply more power to the perimeter groups where the intensity falls off and less power to the center groups where the intensity is more concentrated. Figure 2 shows the lamp group configuration and the location of the solar array with respect to the lamp bank.

The intensity uniformity of the lamp bank was measured by a survey system. Figure 3 shows the plots of the eight reference cells for which the typical intensity uniformity was within ±7 percent. The measuring system automatically traversed eight calibrated reference solar cells in the horizontal direction from one end of the lamp bank to the other. In the vertical direction, the eight reference cells were mounted on an aluminum bar and spanned 25 in. (63.5 cm). Their output was recorded by the survey system's data acquisition system and was plotted in real time against horizontal distance.

Active cooling of the bank was necessary because the nominal wattage of the lamp bank was 20 kW and it was operated in a vacuum. Cooling was accomplished by front panel water cooling and rear panel (lamp sockets) radiation to a –80 °F (–62.2 °C) cold wall (described next).

Cold wall: On the solar array, the heat energy emitted by the lamp bank combined with the heat generated by its electrical operation would raise the operating temperature above the safe limit. To prevent overheating, a recirculating gaseous nitrogen cold wall was located behind the solar array panel and controlled the temperature to –80 °F (–62.2 °C). The low temperature was achieved by introducing liquid nitrogen into the gaseous circulation system. A closed-loop control system was used to achieve temperature stability. Figure 1 shows the location of the cold wall. The maximum temperature of the panel during the test was 100 °F (37.7 °C).

Data Acquisition Systems

The PVPIT utilized three data acquisition systems: steady-state, transient, and plasma density.

Steady-state.—The steady-state data acquisition system architecture was based on the Windows platform and the IEEE–488 bus communicating with various instruments that acquired the data. The software was National Instrument's LabVIEW for Windows. The instruments used were 6 HP 3440lA DMM for voltage and current measurements and a Fluke 2620A data acquisition unit for temperature, solar array floating potential, and bias measurements. In addition, the system also communicated with a Sorensen DCS300 power supply used for biasing the solar array panel above ground and with an HP 6063B programmable load used for loading the solar array panel. Figure 4 shows the system and the various parameters measured. Data acquired were displayed in near real time and were archived. Characteristic plots of solar array current versus voltage I–V were also automatically acquired, displayed, and archived.

Transient.—The transient data acquisition system consisted of a Hi–Techniques multichannel high-speed digitizer controlled by their system software operating on a DOS platform. This system provided sampling rates up to 20 megasamples/sec/channel with an 8-bit resolution. Various voltage and current transients were acquired utilizing Pearson 4100 current transforms, Tektronix A6302/AM503A current probes/amplifiers, and a Tektronix A6902B voltage probe/isolator. Figure 5 shows the system and the various parameters measured.

Plasma diagnostic.—The plasma diagnostic system was a data acquisition system that measured the ion and/or current flow in a Langmuir probe in contact with the plasma. The Langmuir probe is a small metal sphere that collects a charge on its surface. The PVPIT plasma was characterized by using an array of 12 Langmuir probes, 0.75-in. (1.9-cm) stainless steel spheres which were biased with respect to the vacuum facility and used a bipolar power supply. The supply output was driven between ±20 V using a function generator. The probe current was measured by recording the voltage across a 1-kΩ resistor placed between the power supply and the vacuum facility. All supplies were powered using isolation transformers to eliminate ground loops. The data acquisition and control system consisted of a computer-controlled multiplexer tied to a single analog-to-digital converter. This system was designed primarily around the National Instrument's high-speed, 16-bit AT–MIO–16X data acquisition board and their SCXI signal conditioning modules. The software was National Instrument's LabVIEW for Windows. The data acquisition system was menu driven and offered these choices: a selection of probes to collect data, the number of probe characteristics to obtain, and the number of data points to acquire per probe characteristic. Figures 6 and 7 show a simplified and a more detailed block diagram of the system, respectively.

After data were collected, the probe characteristics were reduced using thick-sheath Langmuir probe theory. The validity of this theory was verified by confirming the linear increase in probe current with probe bias in the electron saturation region and by using the results of the analysis to estimate the sheath thickness.

The first phase of the plasma diagnosis was validating the sources and establishing the appropriate operating parameters to provide the desired plasma conditions. Also included were measurements made using all probes to establish the plasma distribution throughout the tank. Tests showed that the plasma density across the array was within the error bar of the Langmuir probe density measurement (a factor of 2 to 3) with no reproducible trends observed. The temperature showed 20-percent fluctuations across the tank, again with no trends worth reporting. When it was clear that a single probe could be used to establish the tank plasma conditions, the probe in the facility center (probe 3) was used to ensure that the plasma conditions were appropriate.

TABLE I.—PLASMA ENVIRONMENT

Date	Time	Electron	
		Temperature, Te, eV	Density, Ne/cm^3
3/16/95	8:30 a.m.	0.15	3×10^6
	12:15 p.m.	.20	5
3/21/95	2:45 p.m.	0.20	3×10^6
	4:00 p.m.	.19	3
3/22/95	12:30 p.m.	0.20	3×10^6
3/23/95	8:10 a.m.	0.17	3.5×10^6
	12:30 p.m.	.20	4
3/29/95	10:00 a.m.	0.19	5×10^6
		.20	5
3/30/95	9:00 a.m.	0.20	5×10^6
	10:00 a.m.	.20	5
4/6/95	3:00 p.m.	0.20	5×10^6

Table I is a listing of the density and temperature measurements for the various test days for probe 3.

Plasma Sources

Two hollow-cathode plasma sources were used to generate a uniform plasma in tank 5. As shown in table I, the resulting plasma had a density of 3 to 5×10^6 electrons/cm^3 and an electron temperature of 0.15 to 0.2 eV, a good simulation of the actual space environment. A third hollow-cathode plasma source was used to simulate a plasma contactor (PC) for the early part of the testing. An actual breadboard plasma contactor was used for the remainder of the testing (fig. 8). Because the plasma contactor is essentially a hollow-cathode plasma source, there was no appreciable difference in the test results with the actual contactor and those with the simulated contactor. Xenon gas was used as the ionized species for all three sources and the contactor.

Photovoltaic Array

One full-size ISS photovoltaic array circuit ("string") consisted of two flight-qualification fidelity panels connected by a flat-collector-circuit (FCC) segment. Figure 9 shows the solar array in its storage box. The total string was composed of 400 cells (200 per panel) in series with bypass diodes across every 8 cells.

Figure 10 shows one PV cell. This configuration results in a potential open-circuit voltage of approximately 240 V and a short-circuit current of approximately 0.96 A. A representative I–V curve is shown in figure 11.

Three-Bay FASTMast

To simulate the station structure during this test, an actual section of the folding articulated square truss mast (FASTMast) was used. The primary on-orbit function of the FASTMast is to support the large flexible solar array blankets. The FASTMast is a mechanism that deploys into a truss structure that is approximately 1296 in. (32.9 m) tall and has a 30.4-in.^{2} (196.1-cm^2) cross section. The on-orbit station structure consists of thirty-two 40.5-in.- (102.9-cm-) tall interconnected bays, each having an upper and lower section and the following principal components: a flexible batten frame, four vertical members called longerons (four upper and four lower per bay), a rigid batten frame, and the wire rope diagonals. The two major components of the flexible batten frame are four fiberglass flexible (flex) battens and four elbow fittings. The flex battens are fiberglass and epoxy pultruded rods. The elbow fittings apply tension to the stainless steel wire rope diagonals from the strained flex battens. The vertical members consist of an upper and lower bay aluminum longeron separated by an elbow fitting. Because of tank size constraints, only three bays of the test article were used in this test. The FASTMast structure is the closest to the solar cell blankets on-orbit and is the most likely to be part of the interaction between the plasma and the real space station array. The three-bay FASTMast is shown in figure 12 and a more detailed description of it is given in reference 2.

Sequential Shunt Unit (SSU) Simulator

An electronic circuit was built to simulate the sequential shunt unit (SSU). This circuit consisted of a field effect transistor (FET) switch with appropriate filtering circuits. The circuit can operate in the frequency range of approximately 10 to 80 kHz.

Test Configurations

During testing, the different system configurations that were required consisted of various connections to the solar array: array negative grounding, positive grounding, various loading, array biasing above and below ground, an SSU inserted between the solar array panel and the load, a connection to the structure, and a plasma contactor to the solar array power lead. Connections for each configuration were made with a coaxial patching panel. Figure 13 shows the system circuit and test configuration.

Test Description and Results

The PVPIT II comprised many individual tests. The following sections present the methods and results of each.

Panel Checkout

Method.—Upon arrival, the solar array panels with the FCC were inspected for damage and were photographed before installation in the vacuum tank. The initial electrical condition of the solar array (a baseline) was obtained by flashtesting, which generates a temperature-corrected I–V curve that characterizes the solar array, including the fill factor. During testing, any degradations in the array due to the vacuum, the plasma, or arcing can be determined by using the baseline I–V curve. The load current is plotted versus the load voltage for an illuminated solar array to generate an I–V curve. The values are determined by varying the load voltage on a solar array (i.e., changing the load resistance) and then by measuring the load current that the array produces. The environmental simulation systems, diagnostics, probes, and data-logging equipment were checked by using the qualification fidelity panels prior to testing. The panels were instrumented with thermocouples so that temperature data could be obtained to interpret plasma results and to model solar array performance.

Results.—Flashtesting was not performed because of equipment failure. Therefore, only comparative I–V curve results using the lamp bank (described in Test Equipment and Environment) were possible.

Initial Conditions

Method.—The following are the actions performed to obtain the initial test conditions.

(1) Environmental simulation equipment (cold wall, lamp bank, plasma sources, and diagnostics) and the test article (solar array) were installed in the vacuum tank. Prior to starting the plasma sources, the tank pressure was measured at 1.1×10^{-6} N/m^2.

(2) A set of four I–V curves was generated without a plasma under a light intensity of approximately 0.38 sun to characterize the solar array. Each curve was generated with a different bias voltage applied: 0, 90, 160, or 200.

(3) The plasma was introduced in the tank and a second set of I–V curves was generated at the same bias voltages as those generated without a plasma. The plasma raised the tank pressure to 4.0×10^{-5} N/m^2. The plasma density and temperature were 3×10^6/electrons/cm^3 and 0.2 eV, respectively.

(4) The positive and negative end voltages of the circuit as it floated in the plasma were measured with noncontacting Trek probes. The floating potential was measured during an I–V curve generation.

Results.—A representative set of I–V curves with and without a plasma are presented in figure 14 and show that the curve shifted when the plasma was introduced into tank 5. What the curve does not show is that the shift was permanent and

remained throughout the testing. One possible explanation for this degradation is that some diffusion pump backstreaming coated the cells. Although the shift may have been significant in an absolute sense, it was insignificant for the PVPIT II, the results of which were only relative because there was no initial flashtest. An example of the floating potential is shown in figure 15.

Plasma-Induced Arcing

Method.—Under steady-state operating conditions (illuminated with no SSU), the array was loaded to 160 and 200 V in sequence, which represents the array's beginning of life (BOL) and end of life (EOL) conditions, respectively. For each load voltage, the array was biased with respect to the plasma so that arcing on the array could be observed under controlled conditions. This biasing allowed the array potential to be adjusted with respect to the plasma (floating potential), and it was set to discrete values within the range of ±200 V. The negative bias voltages were achieved by reversing the bias supply with respect to the positive side of the array.

Figure 16 shows the circuit connections representing the positive orientation of the bias supply. This test was repeated with the array unilluminated to obtain better control of the floating potential. Arc currents could not be measured directly because that would have involved instrumenting the entire surface of the array. Therefore, the currents were measured at the output. Following this test, the tank was brought to atmosphere and the panels were inspected for damage such as the arc marks observed on the photovoltaic array environmental protection (PAEP) panels during PVPIT I.

Results.—A very large number of arcs resulted. The illuminated system stopped arcing with a bias between approximately −115 and 0 V for the 200-V load and less than −50 V for the 160-V load. This equates to a floating potential on the negative side of the array (negative floating potential) of approximately −85 V at a bias of −115 V. When the resulting negative floating potential approached 0 V, arcing was again observed.

Therefore, a plasma contactor that can raise the negative floating potential to not greater than −85 V but to less than 0 V should prevent the array from arcing. The test with the unilluminated array confirmed these results. Figures 17(a), 18(a), and 19(a) show the current, and figures 17(b), 18(b), and 19(b) show the voltage for arcs that occurred with a 200-V bias and a 160-V load.

Figures 20(a) and (b) show the current and voltage, respectively, for an arc with a 200-V bias and no load voltage. Likewise, the photographs in figures 21 and 22 show some of the arc-caused damage to the cell edges. No observable performance degradation in output voltage or current resulted from the arc marks on the cells.

SSU Effects on Plasma Interactions

Method.—The SSU circuit described in Test Equipment and Environment was added to the solar array circuit so that its dynamic response could be observed. The purpose of this test sequence was to determine how the SSU would affect PC operation. Therefore, the load voltage was set to 160 and 200 V prior to the SSU activation so as to represent the full power output condition (no array regulation). The maximum array regulation condition was with the SSU switching at 20 kHz, which resulted in a load voltage of approximately 145 and 176 V, respectively. Other parameters to be measured during this test phase were changes in the arcing rate and magnitude with changes in switching frequency and bias voltage. In this sequence, unlike the previous one, the load voltage (160 or 200 V) was set and maintained while the SSU switching frequency was changed in discrete steps (10, 20, 40, and 80 kHz). The switching frequency remained at each step for a period of time so that arcing transients could be recorded. Following this test, the tank was brought to atmosphere and the panels were inspected for any damage such as the arc marks observed on the PAEP panels during PVPIT I.

Results.—With the SSU switching at 20 kHz, the plasma contactor reduced the negative floating potential of the array for both load voltage conditions, as it was designed to do. The current that the plasma contactor drew from the array appeared to be a linear function of the array load voltage (as the load voltage increased, so did the contactor current). Figure 23 shows the plasma current versus the array load voltage for both load voltage conditions.

Stepping through the switching frequencies proved uninteresting in that no arcing was observed within normal operating conditions. Only when the array was biased so that it electrically floated below −200 V was arcing observed. In addition, while at 40 kHz, the SSU circuit developed a short and the rest of this test sequence was canceled. This decision to cancel was based on the time required to repair the unit and the minimal value that the additional testing would provide.

Plasma Contactor Effects

Method.—A hollow-cathode plasma source was added to the illuminated, loaded solar array circuit (it was operating and a jumper was used to switch it in or out of the circuit as shown in fig. 13). When connected to the circuit, this plasma source functioned as a plasma contactor by shifting the floating potential of the array. Because both the plasma source and contactor are hollow-cathode devices, the plasma source is essentially a plasma contactor. About halfway through testing, an actual breadboard plasma contactor became available. The plasma source was shut down, the plasma contactor was activated and connected to the circuit, and testing was continued. The locations of the plasma source and the contactor differed (fig. 24).

The plasma source was near the bottom corner of the array, closest to the cryopanel, and it fired up toward the array; the plasma contactor was at the opposite end of the array and fired along its center axis towards the cryopanel.

The purpose of this test was to determine whether the plasma contactor was effective in preventing arcing and to examine the effects of its operation on the array. The voltage transients for the positive and negative ends of the arrays as a function of switching in or out of the circuit were recorded; the new steady-state floating potential was measured; and the current to the contactor was measured.

Results.—During the test, the plasma contactor acted quickly to raise the floating potential of the array. The current transients for the positive and negative ends of the array are shown in figure 25.

The plasma contactor only required approximately 130 msec to achieve the desired effect. Figure 26 shows the floating potential shift as the contactor was connected and disconnected from the circuit.

The current that the connected plasma contactor drew from the circuit is shown in figure 27. At an array load voltage of 160 V, the current was approximately 130 mA. This current appeared to be abnormally high for the size of the array in the tank. If the current demand were scaled to the requirements of the entire station (i.e., 82 strings times 6 wings with each string being equivalent to the PVPIT II array), the plasma contactor current would be about 63 A. The high current may have been the result of normal plasma contactor operation and a current loop. By positioning the plasma contactor to fire towards the array, a current loop was established between the array and the plasma contactor.

A second factor contributing to the higher-than-expected currents was the possibility of an array snapover, which occurs when the entire surface of the array, not just the cell edges, becomes conductive to the plasma. A third possible cause for the high current is the high density of neutrals in the tank, on the order of 10^{12} cm^{-3}. If the density were significantly higher near the arrays (i.e., the density in the tank was very nonuniform), then a Paschen discharge could have occurred (ref. 3 and Barbara Gardner and Ira Katz, S-Cubed Division of Maxwell Lab, private communication, June 14, 1995).

Array With FASTMast Structure

Method.—The three-bay FASTMast was electrically bonded to the solar array circuit so that a floating array structure system could be tested in the plasma. Current collected by the FASTMast and the system floating potential were measured. The plasma contactor was introduced in the circuit and the same information as above was recorded. The current collection and arcing threshold potential were evaluated by varying the load resistance and thus the array output voltage.

Results.—Without the contactor, the FASTMast arced rapidly. Arc data were collected as rapidly as the transient data collection system could capture the arcs. The magnitude of these arcs varied from approximately 1.4 to 6.0 A and their duration was about 50 μsec. Figures 28 (1.5 A) and 29 (6 A) are representative of the arcs observed. The array voltage during the 6.0-A arc event is shown in figure 30 (V_{sa}), and the negative and positive array currents during this same arc event are shown in figure 31 (I_{sa}). Arcing ceased when the load voltage was lowered to approximately 65 V. More significantly, arcing also ceased when the plasma contactor was activated (fig. 32).

Out of Eclipse With and Without Plasma Contactor

Method.—The test configuration consists of the solar array circuit with the FASTMast attached and the plasma contactor connected in the circuit as before. The array was illuminated and loaded to 160 V to establish the load voltage setting. Next, the lamp bank was turned off without changing any load settings, and the change in floating potential, structure current, and other system parameters was recorded. This darkening of the array was to simulate going into the eclipse portion of an orbit. The array was then illuminated and the voltage and current transients recorded along with the new steady-state floating potential. The illumination was to simulate coming out of eclipse. Both simulations were performed with the contactor switched out of the circuit and then were repeated with the contactor switched in. The current to the contactor was measured during the testing sequence.

Results.—As a result of limitations on the lamp bank power supplies and controls, it could not be switched on instantaneously, only gradually over a matter of seconds. Shutting off power to the lamp bank was instantaneous, but because they took some time to darken, the lights were very hot. Therefore, the only data that could even be considered true transient data were those during the eclipse simulation. Because of these considerations, no transient data were recorded. Figure 33 shows the contactor currents during the simulations, and they are consistent with those previously measured.

Out of Eclipse With and Without SSU Circuit

Method.—The previous test (with and without the plasma contactor) was repeated, except that the SSU was added to the circuit and was switched on and off.

Results.—This test was similar to the preceding one in that it had the same problems simulating eclipse and illumination transients. Unlike that test, data were collected for arcing transients when the contactor was not activated. Some of these arcing events are shown in figures 34 and 35. Figure 36 is an arc without the SSU switching, and figure 37 is an arc with a 20-kHz SSU switching.

Final Conditions

Method.— A final set of I–V curves was generated first with the plasma sources on and then with them off. When the plasma sources were still on, the ground polarity of the system was switched from negative to positive to study the effects of ground polarity on arcing. Early in the Space Station Freedom program, a positive ground was proposed to eliminate arcing but was rejected for programmatic reasons. After removal from the vacuum tank, the solar array panels and FCC were inspected for damage and were photographed to document the changes undergone during the previous testing.

Results.—As seen from figure 38, the plasma contactor caused an expected decrease in the power output of the array. Also of interest in the figure is that when the system was positively grounded, the power output was almost the same as that when the system was operating without a plasma. Furthermore, there was no arcing with a positive ground regardless of the array output voltage (i.e., all the way to open-circuit voltage).

Test Comparability

Method.—To determine the differences in current requirements in PVPIT I and PVPIT II, cover glass overhangs were measured. However, because of logistical problems, measurements of the test article could not be made. Instead, measurements were made on a 16-cell coupon (Nadeem Rahman, summer intern student at the NASA Lewis Research Center, private communication, July, 1995) that was built using the same process controls as the test article so as to achieve consistency in cover glass alignment. These coupon measurements were then compared with those of the PVPIT I test article.

Results.—The average overhangs were similar: 0.0048 for the coupon and 0.0045 for the PVPIT I test article. Therefore, the overhang is not a significant source of the differences in the PVPIT I and PVPIT II results. Of course, the variance in the individual overhangs and any actual differences in the coupon and the PVPIT II test article are still factors. When examined, the amount of cover glass overhang was comparable in PVIT I and PVIT II. Therefore, this fails to explain the differences between the test results.

Concluding Remarks

During the testing, the current requirements of the plasma contactor were very large relative to the expected levels and may be attributed to three causes, the first of which is that the array snapped over at about 150 V. The second is that a current loop may have been established between the plasma contactor and the array. Therefore, the on-orbit currents should be far less than what this test indicated. The controlling factor in both of the preceding is the amount of cover glass overhang.

The third cause of the plasma contactor high current requirements was an abnormally high density of neutral xenon that surrounded the array during testing. Such a density, if sufficiently high, could create a Paschen discharge, which would have the same effect as that in a Crookes tube (a fluorescent tube).

Regardless of the cause of the excess current, the plasma contactor lowered the floating potential of the structure and thus reduced and/or eliminated arcing.

Recommendations

The following recommendations are made on the basis of the test results:

1. Position the contactor so that it does not fire into the arrays, thus avoiding the creation of a current loop.
2. Model the tank test to better understand the results of this test.
3. Measure the amount the cover glass overhangs the flight articles so as to prevent exposed cell edges.

Lewis Research Center
National Aeronautics and Space Administration
Cleveland, Ohio, September 30, 1996

Appendix—Acronyms

BOL	beginning of life conditions
EOL	end of life conditions
FASTMast	folding articulated square truss mast
FCC	flat collector circuit
FET	field effect transistor
ISS	International Space Station
LEO	low-Earth orbit
PAEP	photovoltaic array environmental protection
PC	plasma contactor
PV	photovoltaic
PVPIT	photovoltaic plasma interaction test
SSF	Space Station Freedom
SSU	sequential shunt unit
TCA	test cage assembly

References

1. Felder, M.C., et al.: Results of Testing Conducted in Tank 5 for Interactions Between Space Station Freedom and Plasma. NASA Lewis PIR#268, Jan. 22, 1993.
2. Shaker, J.F.: Static Stability of a Three-Dimensional Space Truss. NASA TM–106944, 1995.
3. Cobine, J.D.: Gaseous Conductors: Theory and Engineering Application. Dover Publications, Inc., New York, 1958.

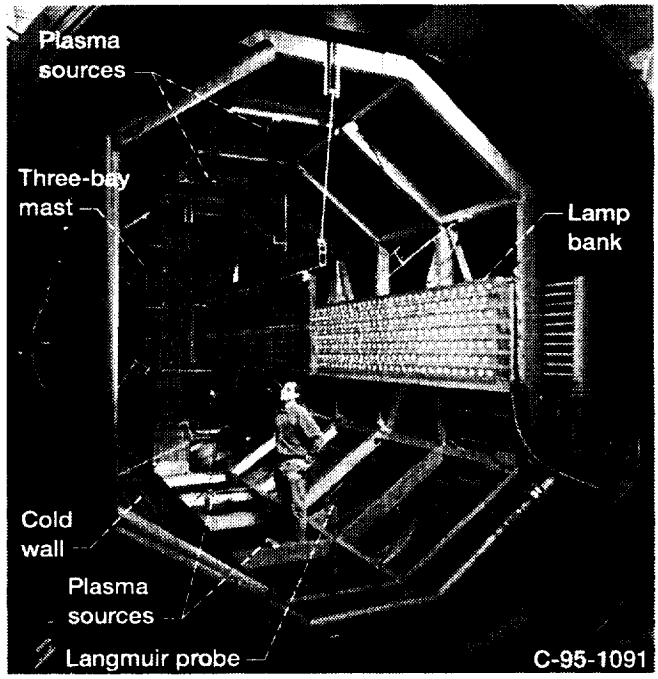

Figure 1.—Test cage assembly in tank 5.

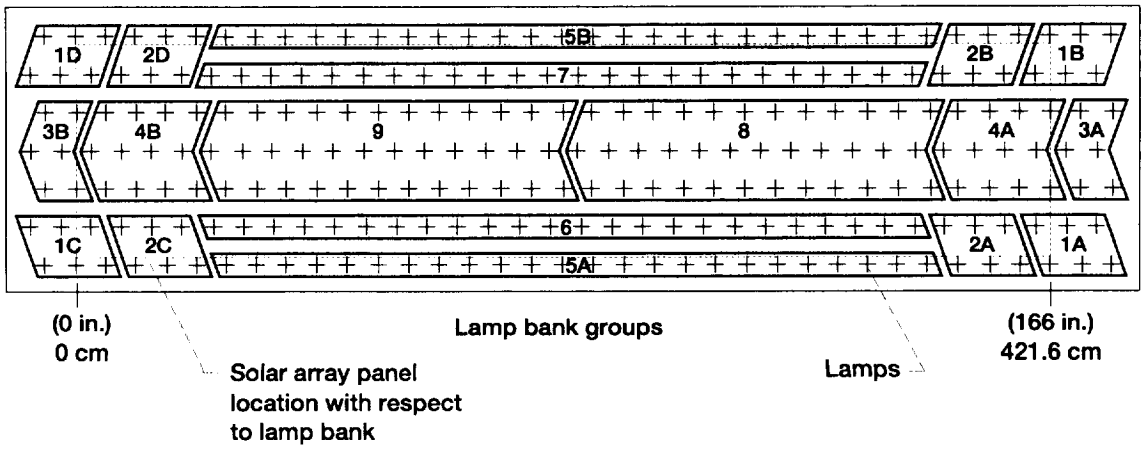

Figure 2.—Lamp bank layout.

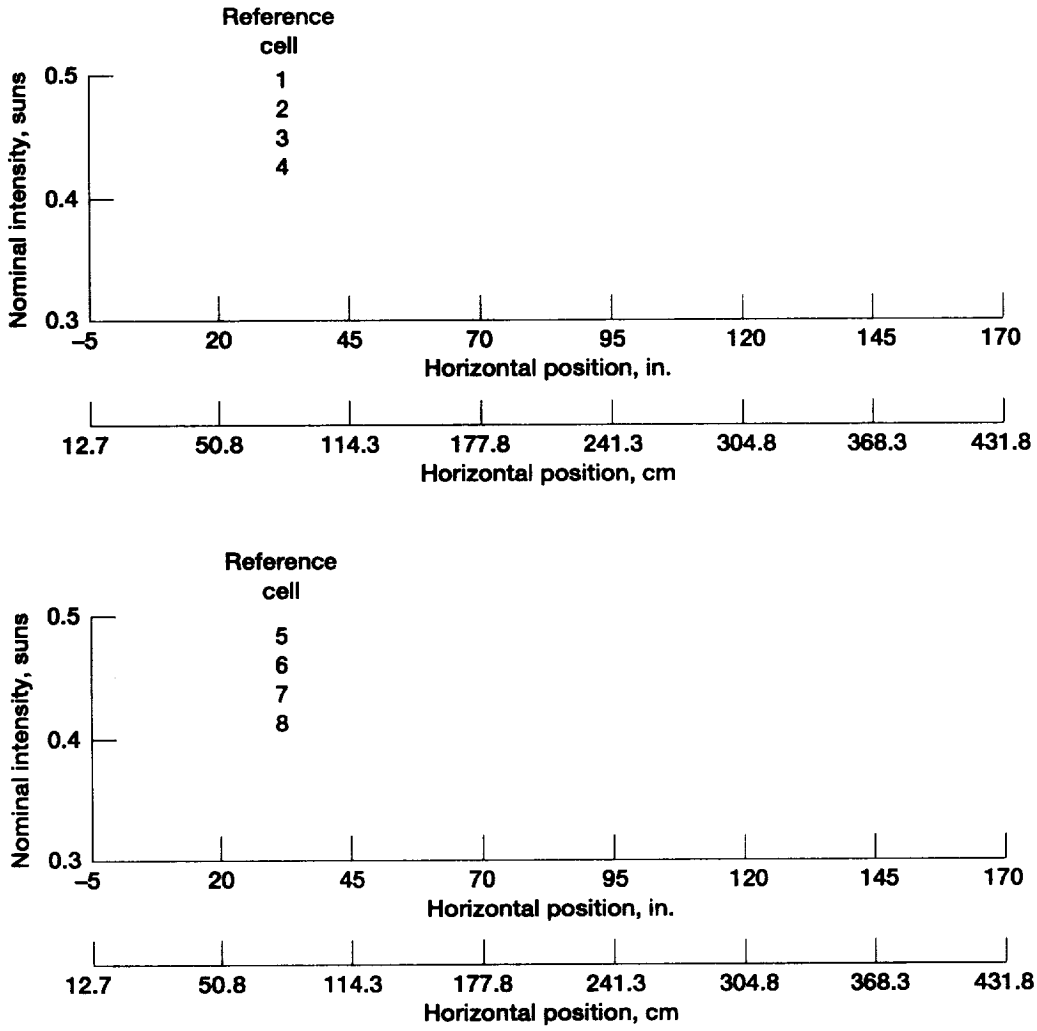

Figure 3.—Lamp bank intensity uniformity.

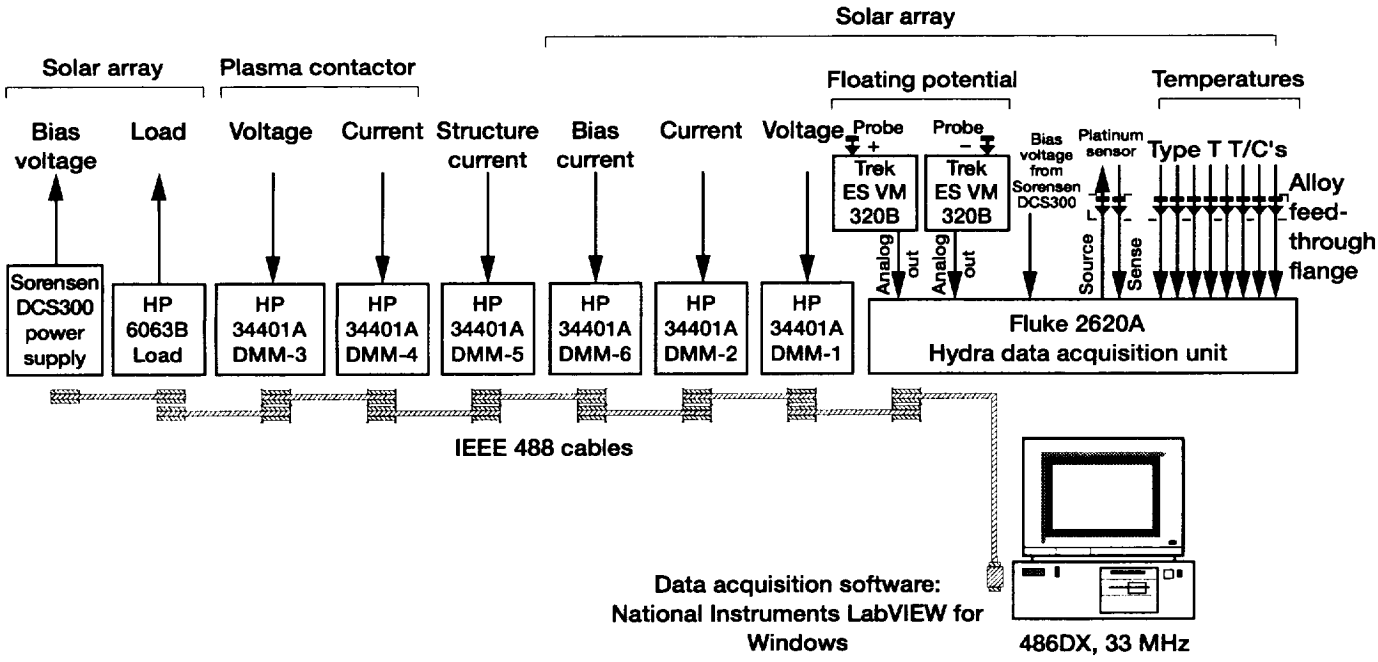

Figure 4.—Steady-state data.

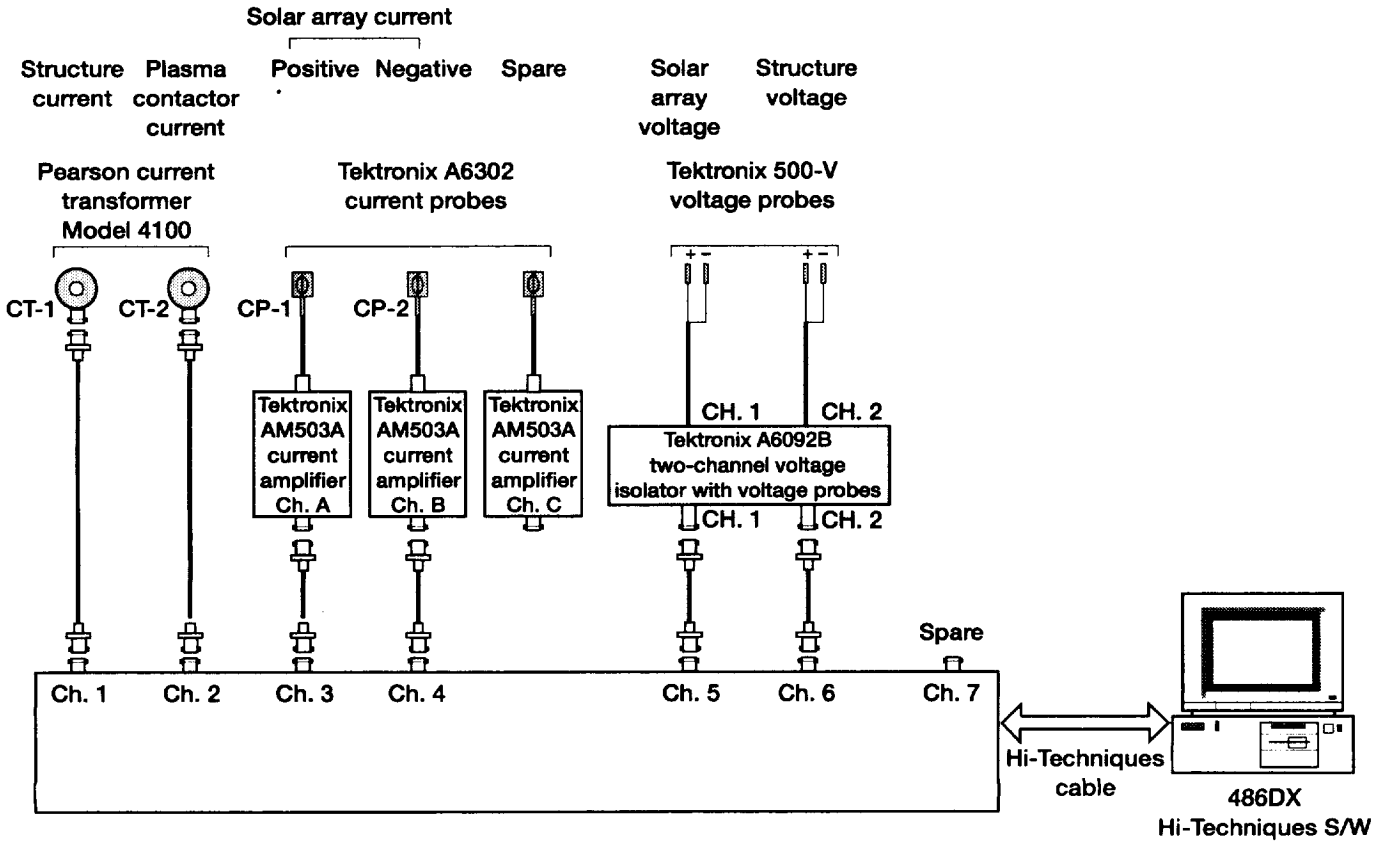

Figure 5.—Transient data acquisition system.

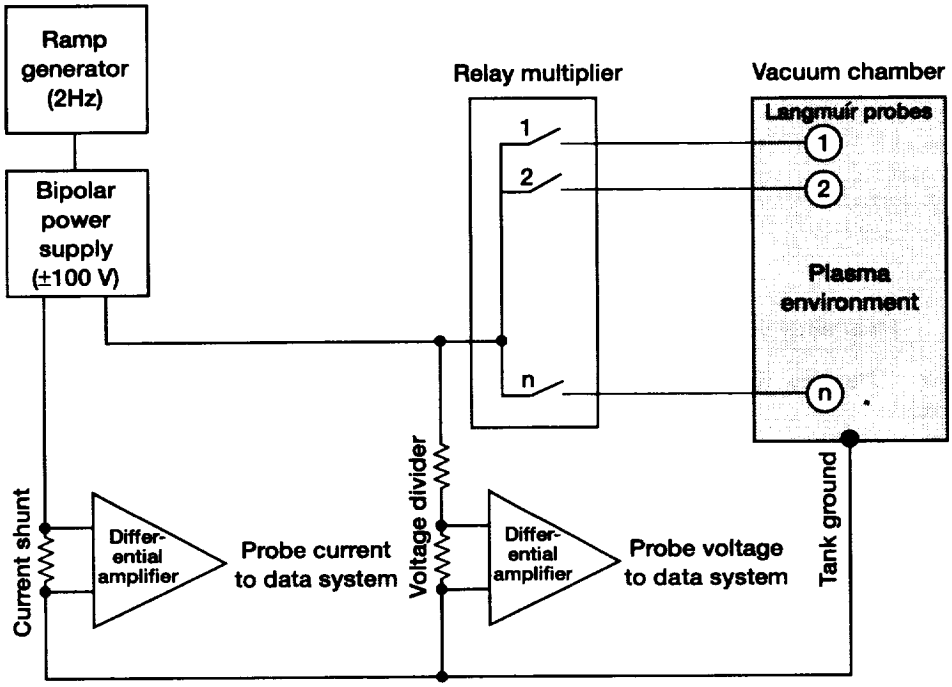

Figure 6.—Plasma diagnostics (simplified).

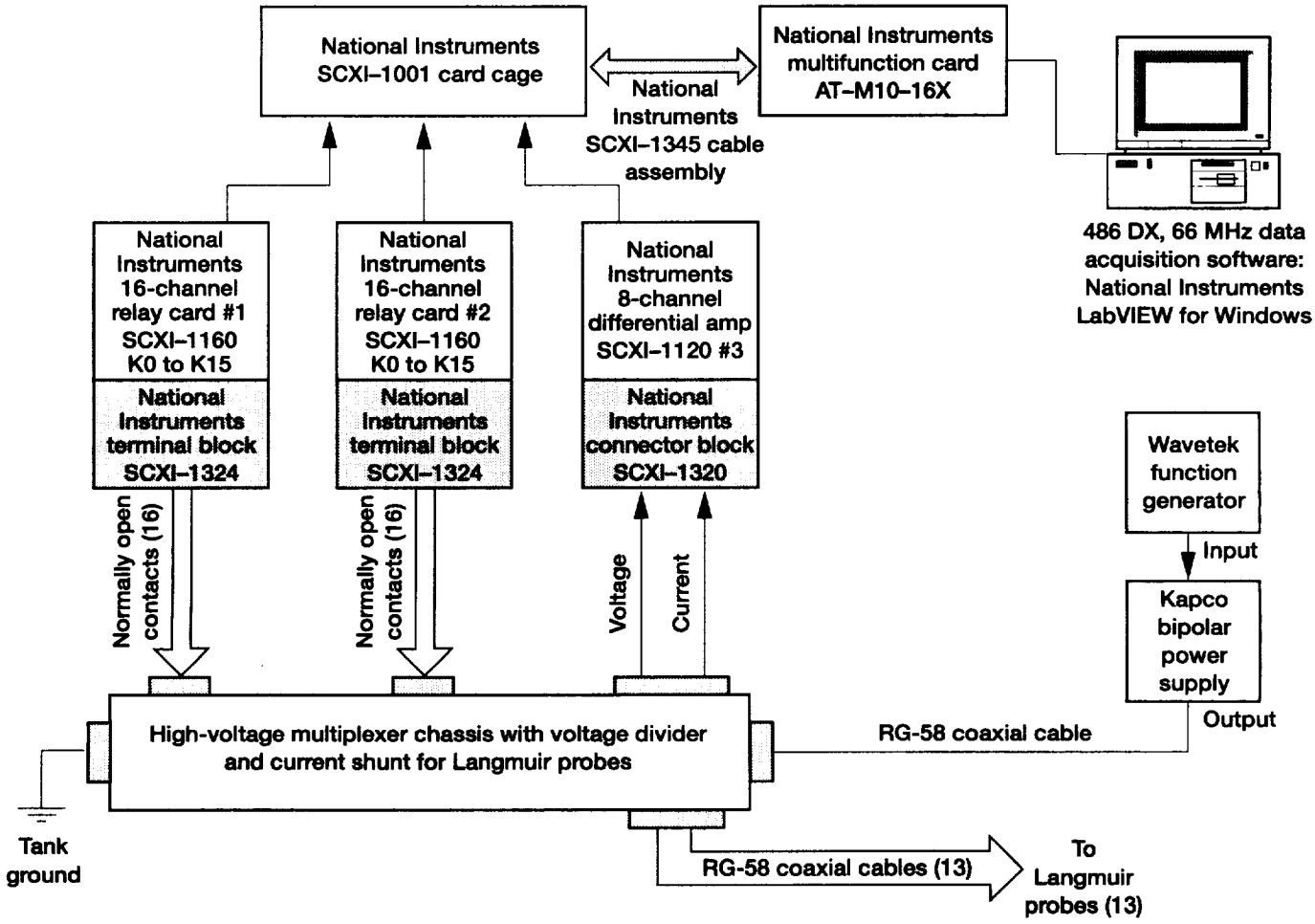

Figure 7.—Plasma diagnostics (detailed).

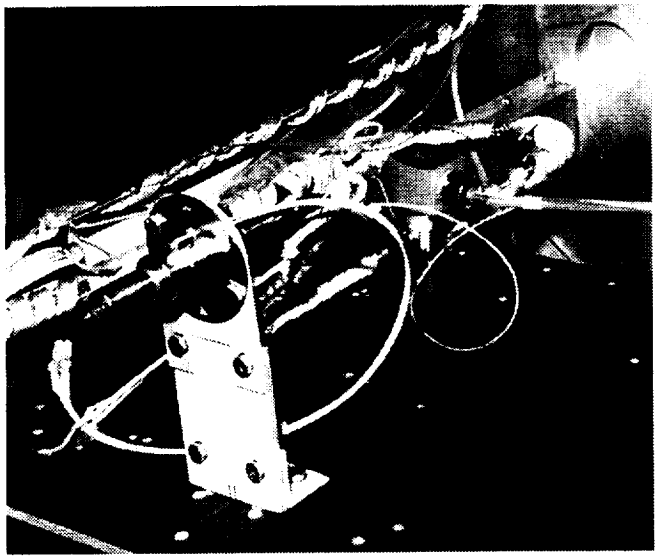

Figure 8.—Plasma contactor.

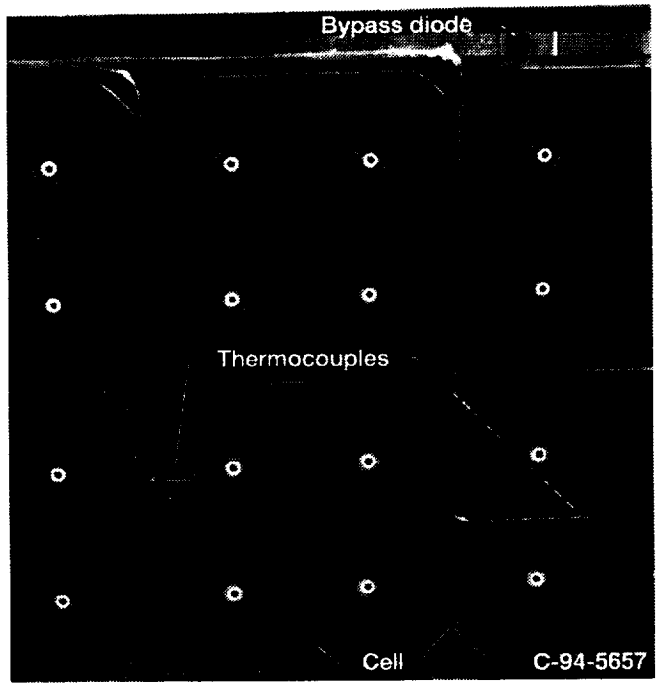

Figure 10.—Photovoltaic cell.

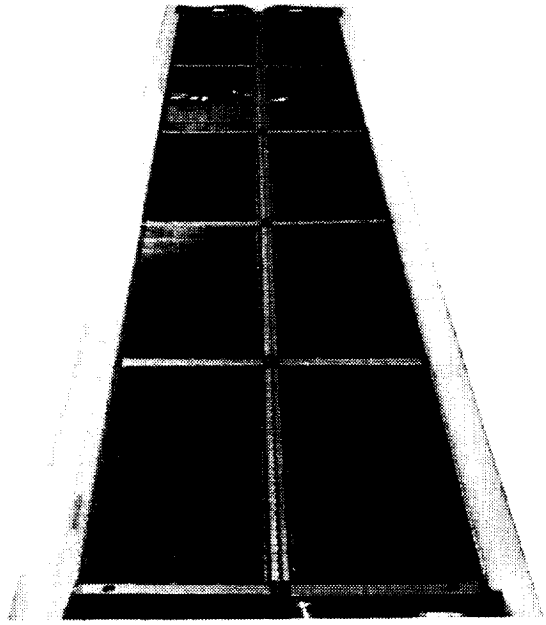

C-94-3602

Figure 9.—Solar array in storage box.

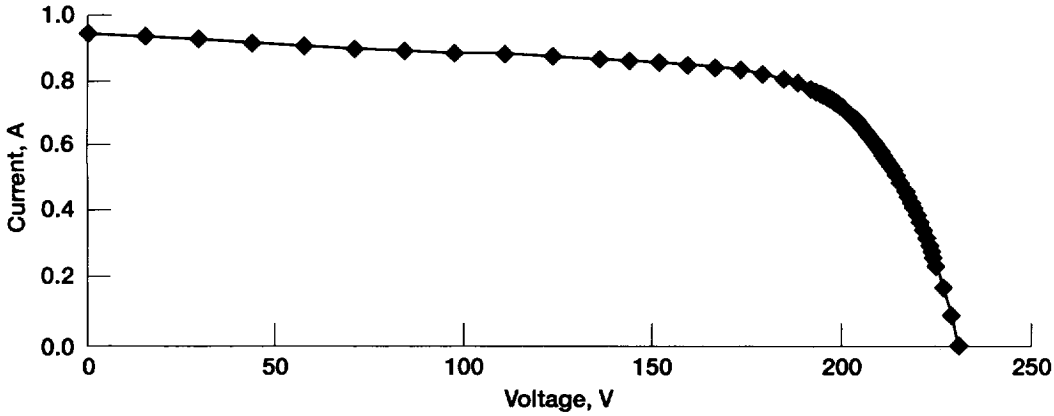

Figure 11.—Array I–V curve.

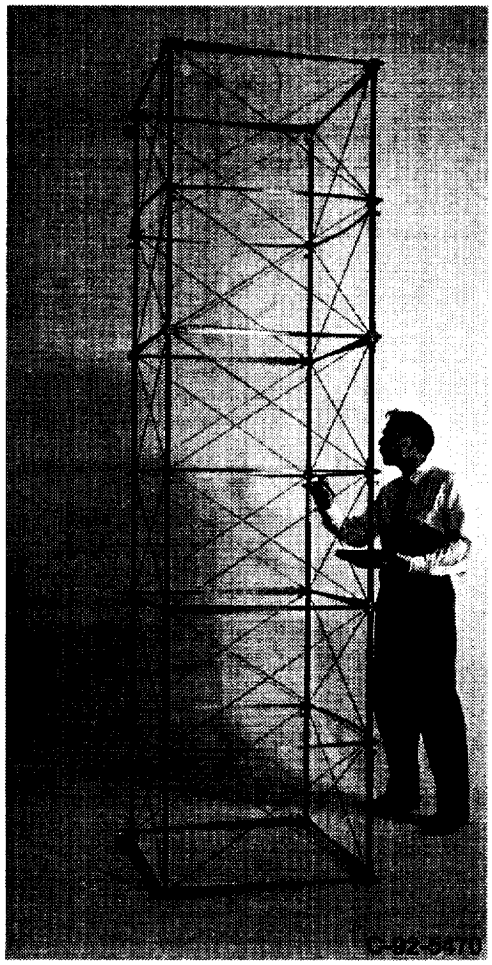

Figure 12.—FASTMast.

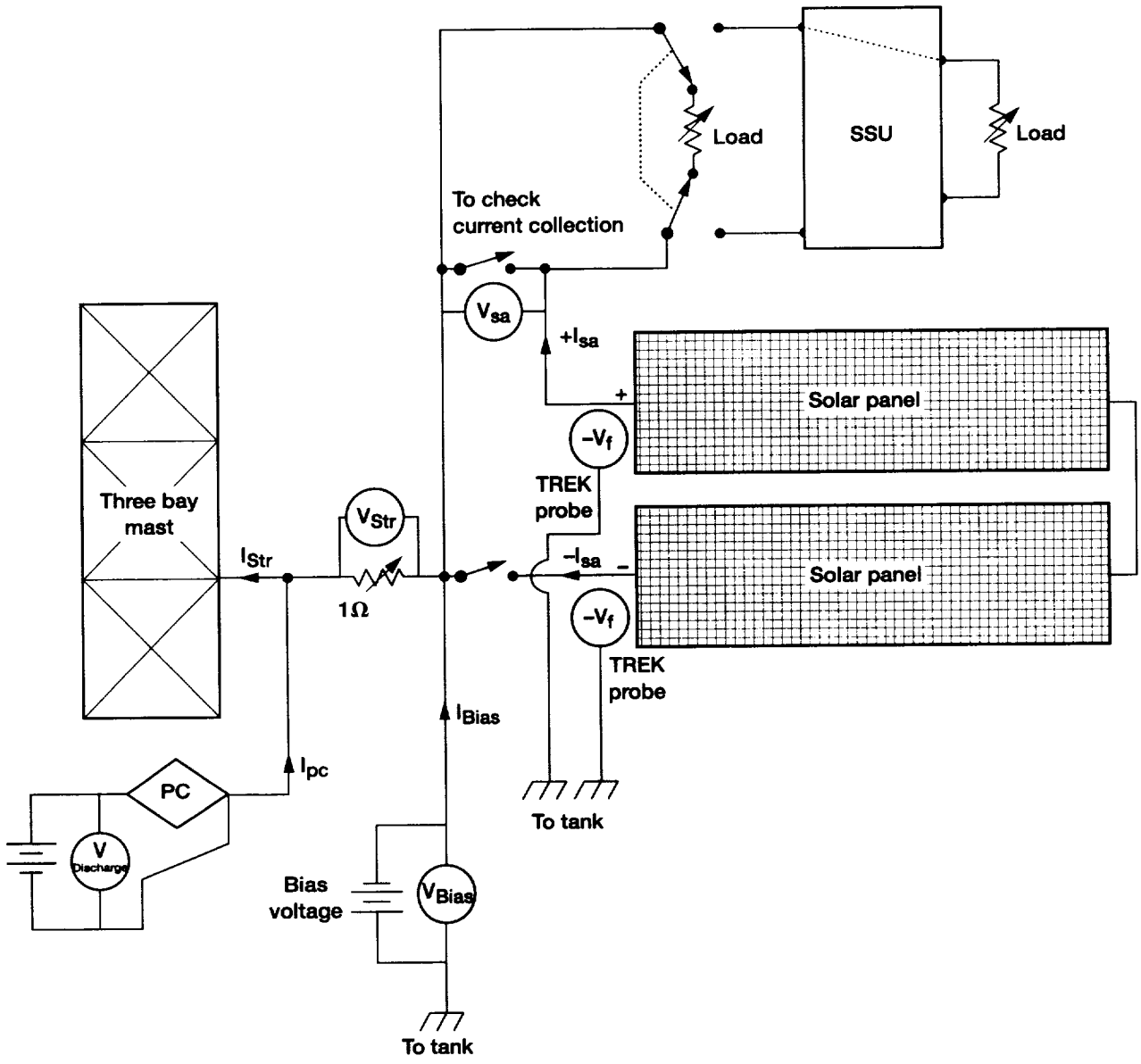

Figure 13.—System test configuration.

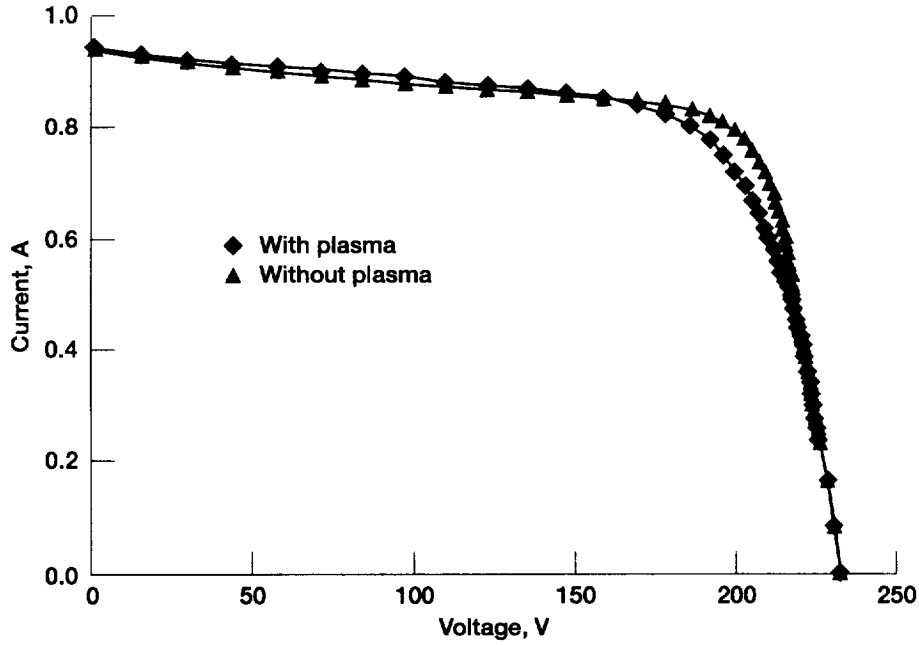

Figure 14.—Initial conditions. Bias voltage, 90.

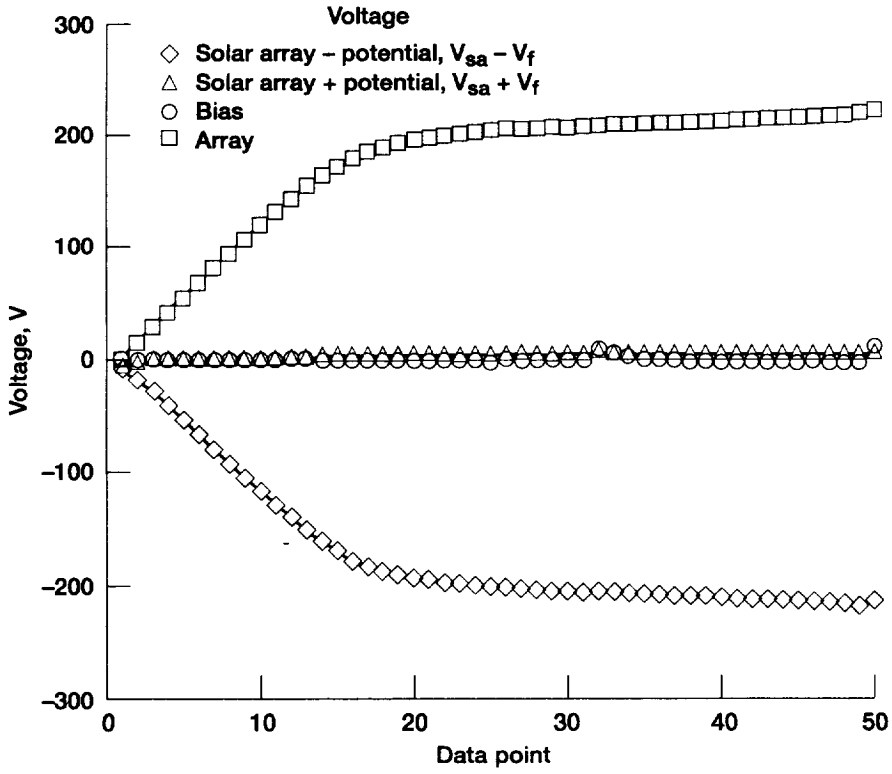

Figure 15.—Floating potentials.

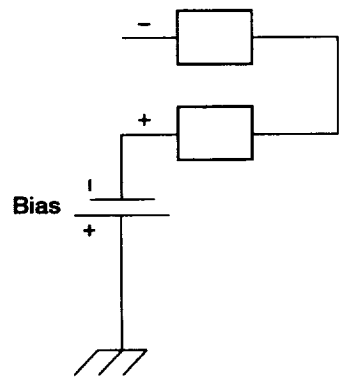

Figure 16.—Bias supply positive orientation for testing.

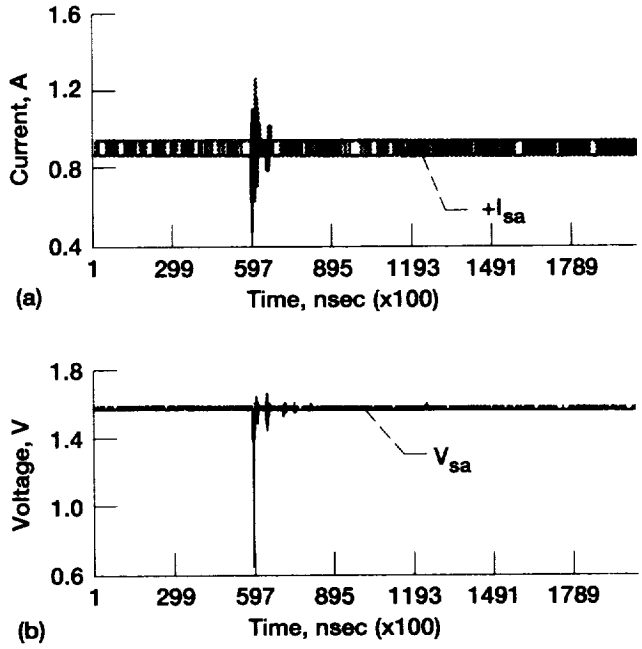

Figure 18.—Arc at 200-V bias and 160-V load. (a) Structure current; $+I_{sa}$, positive side of array. (b) Array voltage, V_{sa}.

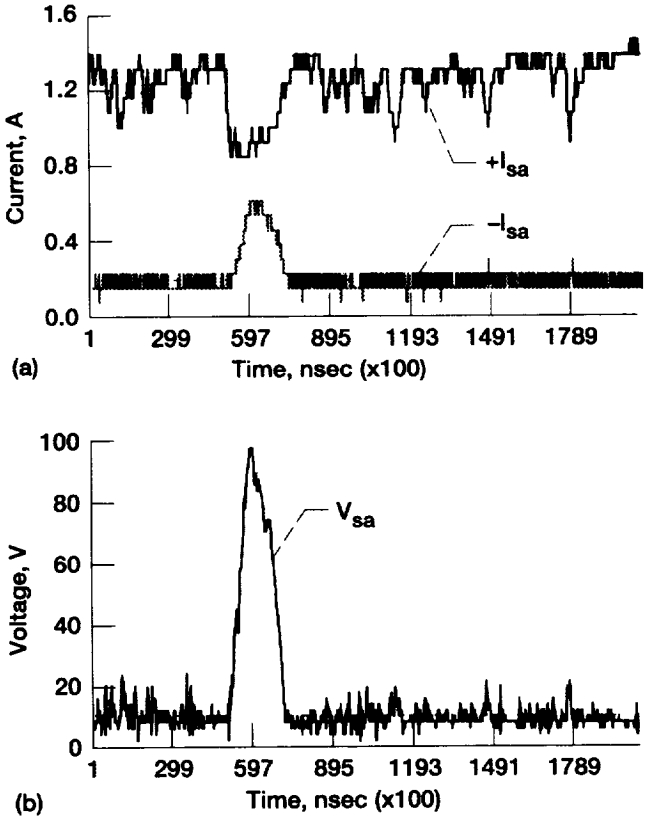

Figure 17.—Arc at 200-V bias and 160-V load. (a) Structure current; $+I_{sa}$, positive side of array; $-I_{sa}$, negative side of array. (b) Array voltage, V_{sa}.

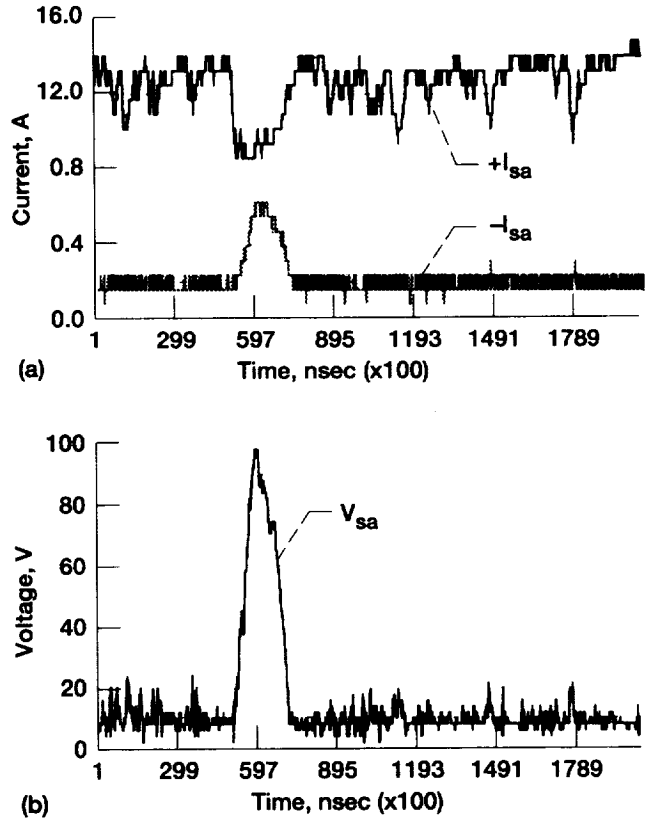

Figure 19.—Arc at 200-V bias and 160-V load. (a) Array current; $+I_{sa}$, positive side of array; $-I_{sa}$, negative side of array. (b) Array voltage, V_{sa}.

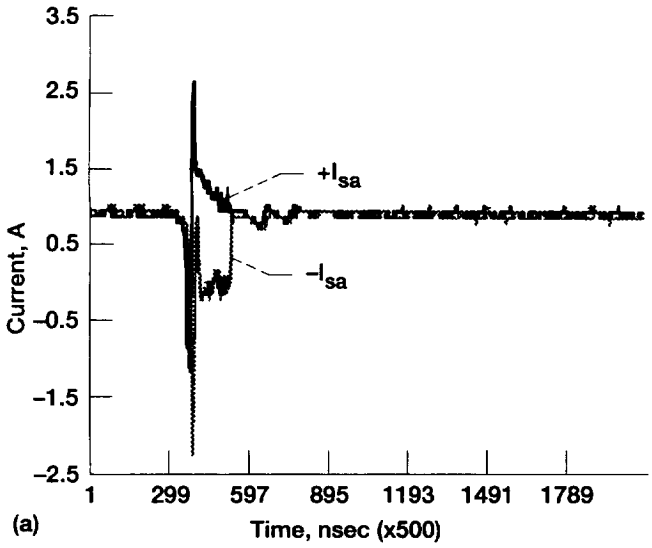

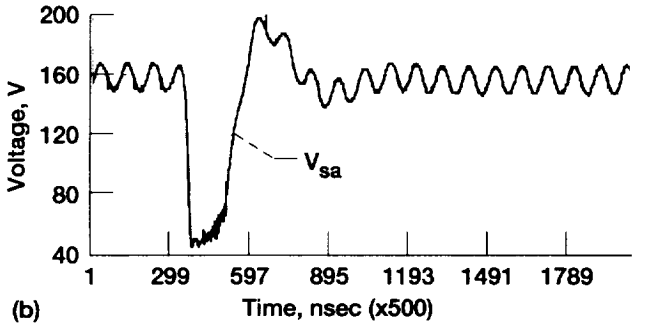

Figure 20.—Arc at 200-V bias and no load voltage. (a) Array current; $+I_{sa}$, positive side of array; $-I_{sa}$, negative side of array. (b) Array voltage, V_{sa}.

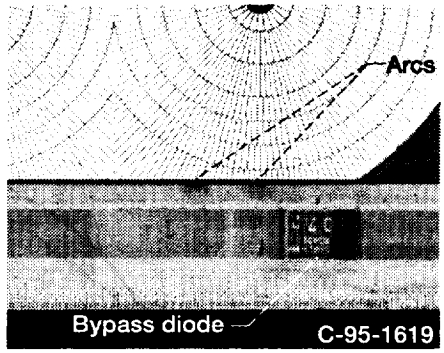

Figure 21.—Cell edge damage (negative image for clarity).

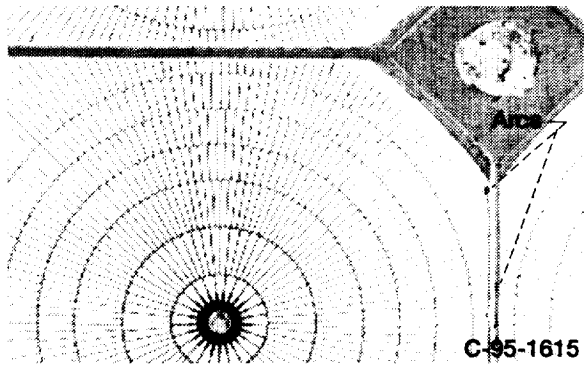

Figure 22.—Cell edge damage (negative image for clarity).

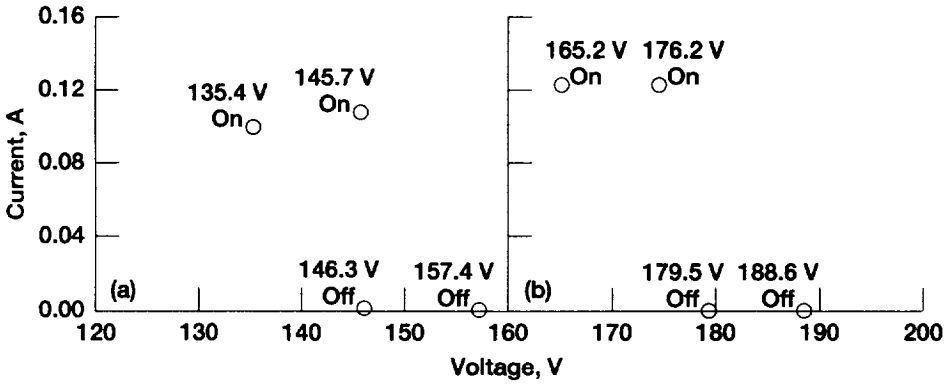

Figure 23.—Contactor current requirements with SSU. (a) 160-V unregulated voltage. (b) 200-V unregulated voltage.

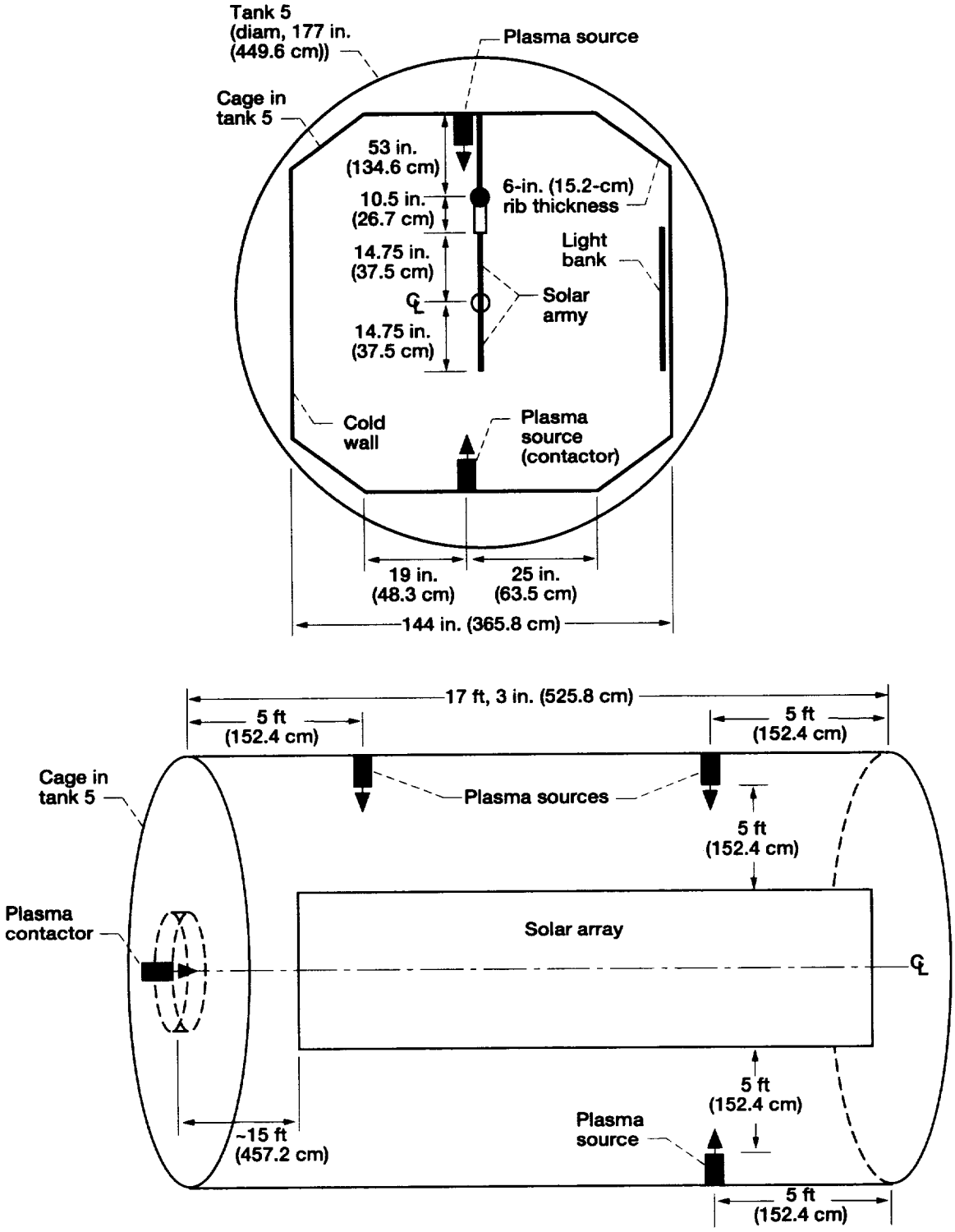

Figure 24.—Contactor and source locations. Note: drawing not to scale; plasma source was only used as a plasma contactor for first part of test and was never used to provide plasma environment.

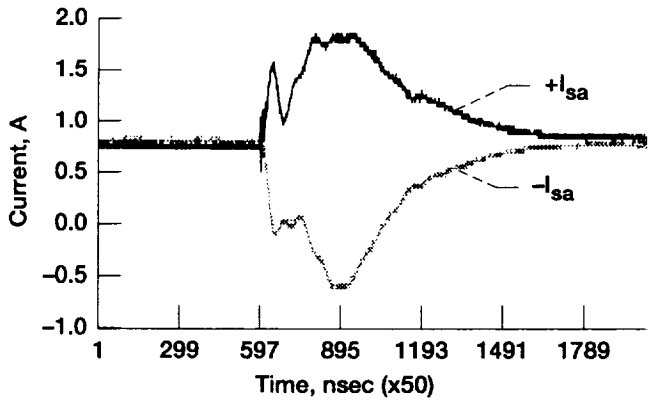

Figure 25.—Array voltage during arc. Array current; $+I_{sa}$, positive side of array; $-I_{sa}$, negative side of array.

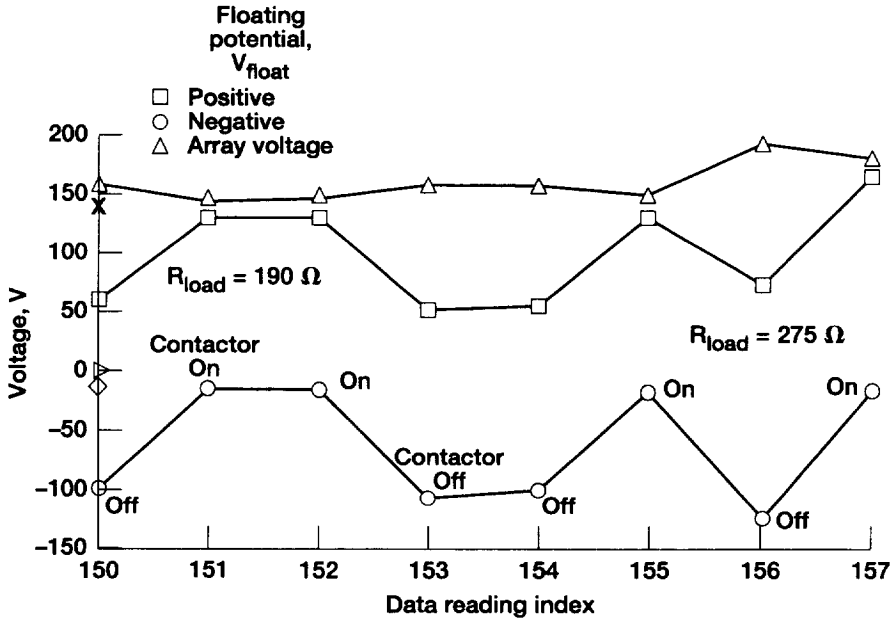

Figure 26.—Floating potentials.

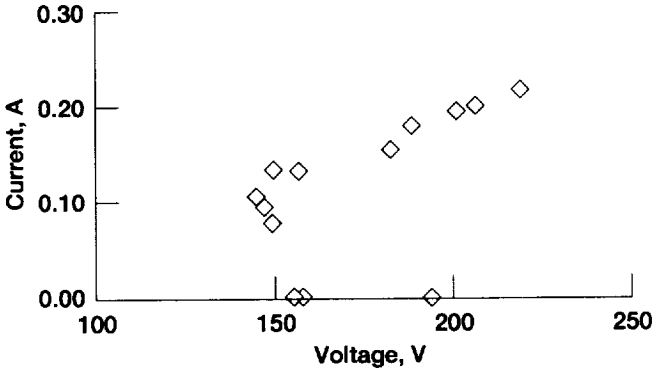

Figure 27.—Contactor current.

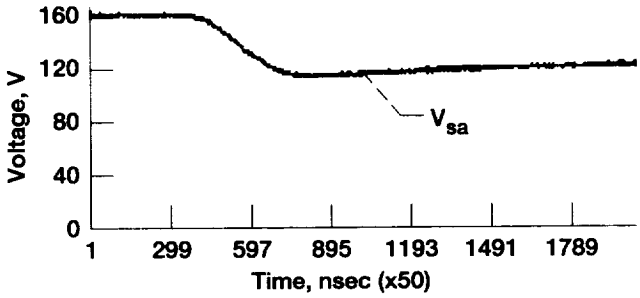

Figure 30.—Array voltage during arc.

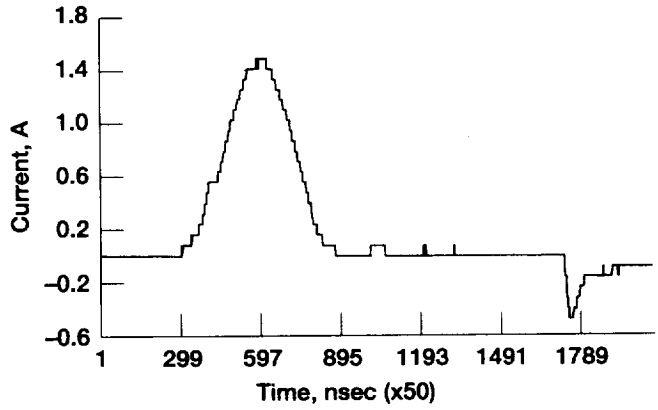

Figure 28.—Small arc.

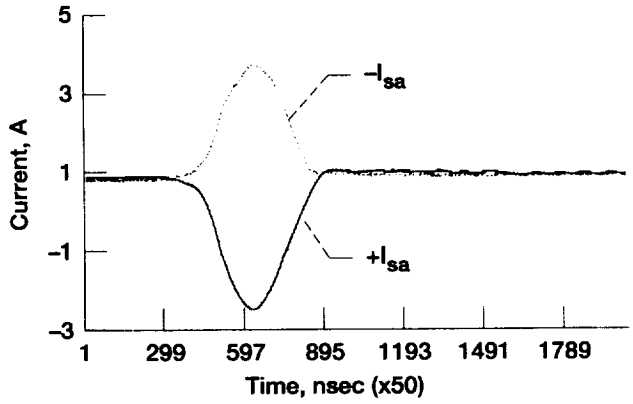

Figure 31.—Array current during arc.

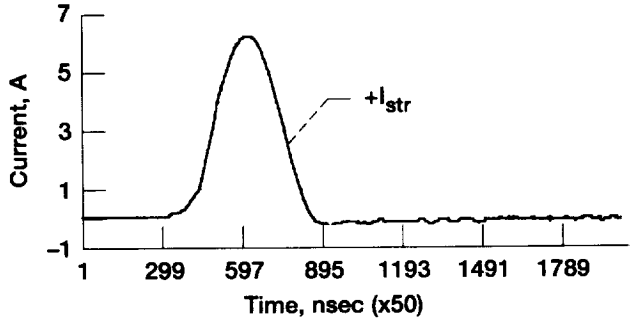

Figure 29.—Large arc.

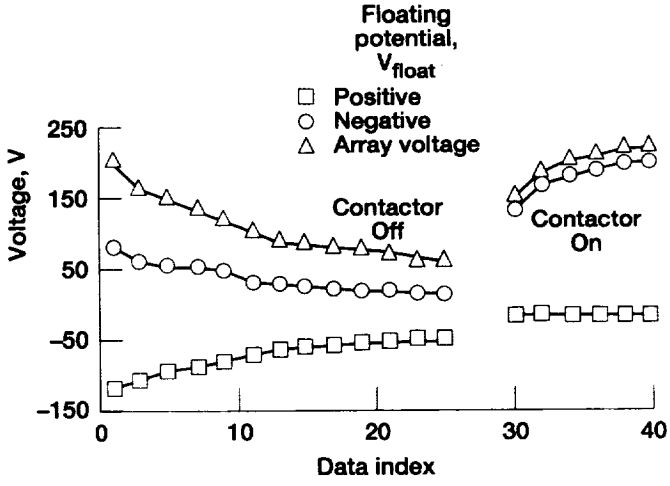

Figure 32.—Constant negative floating potential with contactor.

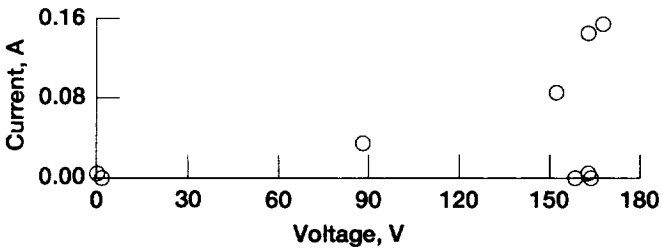

Figure 33.—Contactor current versus array voltage in and out of eclipse.

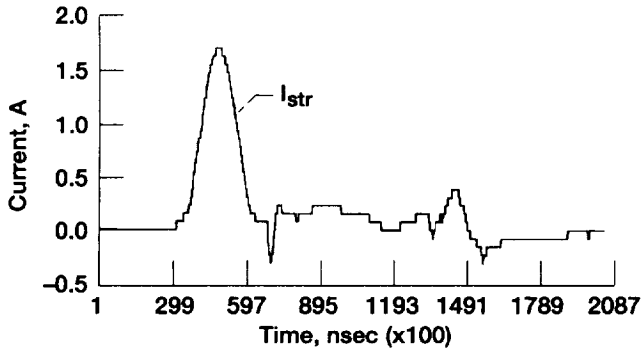

Figure 34.—Arc example 1.

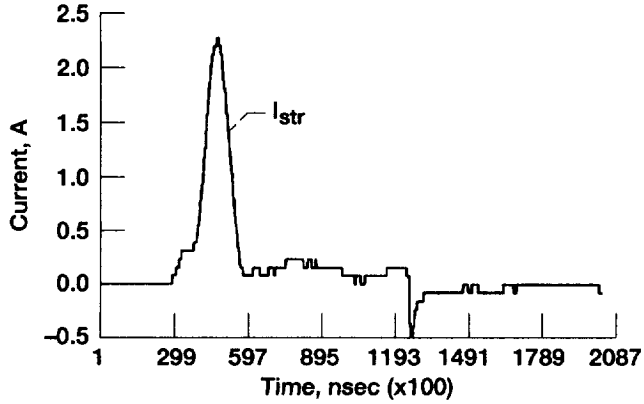

Figure 35.—Arc example 2.

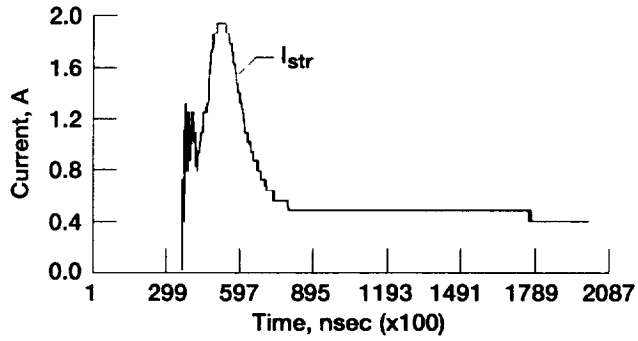

Figure 36.—Arc without sequential shunt unit (SSU).

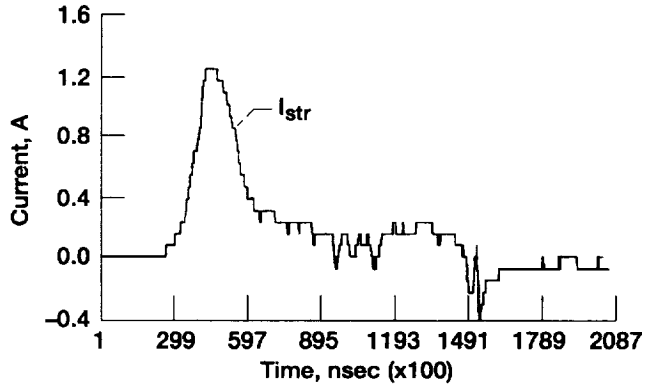

Figure 37.—Arc with sequential shunt unit (SSU).

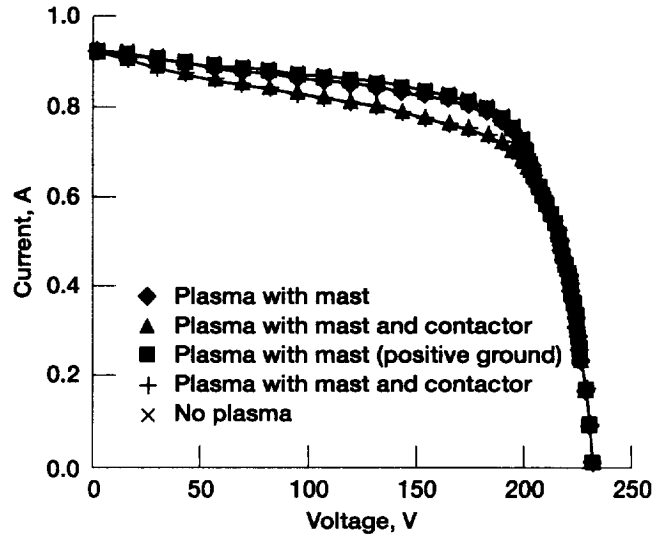

Figure 38.—Operation comparison.

REPORT DOCUMENTATION PAGE

Form Approved
OMB No. 0704-0188

Public reporting burden for this collection of information is estimated to average 1 hour per response, including the time for reviewing instructions, searching existing data sources, gathering and maintaining the data needed, and completing and reviewing the collection of information. Send comments regarding this burden estimate or any other aspect of this collection of information, including suggestions for reducing this burden, to Washington Headquarters Services, Directorate for Information Operations and Reports, 1215 Jefferson Davis Highway, Suite 1204, Arlington, VA 22202-4302, and to the Office of Management and Budget, Paperwork Reduction Project (0704-0188), Washington, DC 20503.

1. AGENCY USE ONLY (*Leave blank*)	2. REPORT DATE	3. REPORT TYPE AND DATES COVERED
	December 1996	Technical Paper

4. TITLE AND SUBTITLE

Photovoltaic Plasma Interaction Test II

5. FUNDING NUMBERS

WU-478-42-10

6. AUTHOR(S)

Bradford A. Kaufman, Daniel Chrulski, and Roger M. Myers

7. PERFORMING ORGANIZATION NAME(S) AND ADDRESS(ES)

National Aeronautics and Space Administration
Lewis Research Center
Cleveland, Ohio 44135-3191

8. PERFORMING ORGANIZATION REPORT NUMBER

E-10332

9. SPONSORING/MONITORING AGENCY NAME(S) AND ADDRESS(ES)

National Aeronautics and Space Administration
Washington, D.C. 20546-0001

10. SPONSORING/MONITORING AGENCY REPORT NUMBER

NASA TP-3635

11. SUPPLEMENTARY NOTES

Bradford A. Kaufman and Daniel Chrulski, NASA Lewis Research Center; Roger M. Myers, NYMA, Inc., 2001 Aerospace Parkway, Brook Park, Ohio 44142 (work performed under NASA Contract NAS3-27186). Responsible person, Bradford A. Kaufman, organization code 5450, (216) 433-5636.

12a. DISTRIBUTION/AVAILABILITY STATEMENT

Unclassified - Unlimited
Subject Category 46

This publication is available from the NASA Center for AeroSpace Information, (301) 621-0390.

12b. DISTRIBUTION CODE

13. ABSTRACT ***(Maximum 200 words)***

The International Space Station (ISS) program is developing a plasma contactor to mitigate the harmful effects of charge collection on the station's large photovoltaic arrays. The purpose of the present test was to examine the effects of charge collection on the solar array electrical circuit and to verify the effectiveness of the plasma contactor. The results showed that the plasma contactor was able to eliminate structure arcing for any array output voltage. However, the current requirements of the plasma contactor were higher than those for prior testing and predicted by analysis. Three possible causes for this excess current demand are discussed. The most likely appeared to be a high local pressure on or very near the surface of the array as a result of vacuum tank conditions. Therefore, in actual space conditions, the plasma contactor should work as predicted.

14. SUBJECT TERMS

Photovoltaic; PV; Plasma interactions; Space station; Power systems

15. NUMBER OF PAGES

27

16. PRICE CODE

A03

17. SECURITY CLASSIFICATION OF REPORT	18. SECURITY CLASSIFICATION OF THIS PAGE	19. SECURITY CLASSIFICATION OF ABSTRACT	20. LIMITATION OF ABSTRACT
Unclassified	Unclassified	Unclassified	